Journal of Engineering Science and Technology Review 16 (1) (2023) 186 - 196

Research Article

JOURNAL OF
Engineering Science and Technology Review

www.jestr.org

Proposal for Improving Power Quality in Brazilian Navy Ships through the Application of Shunt Active Power Filters (SAPF)

André Tiago Queiroz[1], Angelo Cesar Colombini[1], Elvanger Santos Cardoso[1], Márcio Zamboti Fortes[1,*], Paulo Roberto Duailibe Monteiro[1] and Rodrigo Henrique Cunha Palácios[2]

[1] *Engineering School, Fluminense Federal University, Niteroi, Brazil*
[2] *Academic Department of Computing, Technological Federal University of Paraná, Paraná, Brazil*

Received 13 December 2022; Accepted 27 February 2023

Abstract

This article presents the results of a simulation of the electrical system of the *"Corveta Classe Barroso"* or *CCB*, a ship in the Brazilian Navy, using the MATLAB program. The objective of the simulation is to measure, evaluate, and mitigate the harmonics at the output terminals of the ship's generator group, driven by the non-linear loads connected to the Point of Common Coupling (PCC) of the distribution system, such as three-phase Static Rectifiers, Specific Loads, and a Water-Cooling Unit. The simulation was divided into two stages, with the first stage simulating the system without the presence of the Shunt Active Power Filter (SAPF) and the second stage including the SAPF. The design of the SAPF was based on the IRP p-q theory, and it was found that the SAPF was effective in reducing current and voltage distortions, improving the true power factor, reducing harmonic pollution, and reducing voltage modulation. The results obtained during the second stage of the simulation that considered the presence of the SAPF indicated that the aforementioned filter was an adequate choice for improving the power quality of the ship under study.

Keywords: Total Harmonic Distortion, Shunt Active Power Filter, Ship, Power factor, Electrical Power System.

1. Introduction

The Brazilian Navy Ship is equipped with several equipment and sensors of high technological complexity; therefore, it is necessary that a good quality of electrical energy is generated on board to ensure that the availability, the reliability and the efficiency of such devices are maintained during the entire period of operation [1,2,3]. In this way, the energy generated on board the Barroso Class Corvette (*Corveta Classe Barroso or CCB*) must remain stabilized and with its harmonic distortions within the limits established in the current regulations [4,5,6,7,8], thus contributing to navigation safety and for the measurement accuracy of targets and contacts collected by on-board equipment, whether high speed (missiles and aircraft) or low speed (ship and submarine).

The Active Power Filters (APF), despite having a high implementation cost and high operational complexity in electrical projects, have been shown to be a more assertive option to improve the compensation of harmonic components, frequency range diversity, factor correction of power (FP) , among other parameters that can contribute to the improvement of the electric power quality (EPQ) generated in the referred vessel. Given the characteristics and advantages of these types of devices, in this work, the harmonic mitigation modality is based on Shunt Active Power Filters (SAPF) [9,10,11,12,13,14]. The SAPF can be considered an electronic converter that can inject harmonic components into the system to which it is installed the necessary harmonic components to cancel unwanted current harmonics generated at the terminals of non-linear loads. Thus, in order to cancel the aforementioned harmonics, the SAPF are installed at the Point Common Coupling (PCC) of system of an alternating current (AC) to compensate one or several loads. Once installed, the harmonic flow of current to the system is limited. In addition to compensating current harmonics, SAPF can also be used to compensate for reactive power, current imbalance, negative sequence current [11,12,13,14].

2. Theoretical Background

This chapter aims to present the main theories consulted and used during the research, and which, in some way, contributed to the evaluation and analysis of the results, serving as a basis for the modeling and simulation of the Generation, Distribution, and Consumption Systems of the CBB, as well as helping in the development of the SAPF project. Therefore, it becomes necessary to define and address some quantities considered important in this work, so we have:

Voltage Modulation (VM): is the periodic variation of the voltage $(\Delta_V/2)$ allowed by the user in relation to the rated voltage (V_n). The VM periodicity is considered greater than one cycle and less than 10 seconds [4].

$$\mathrm{VM} = \frac{\Delta_V}{2*Vn} = \frac{Vmax-Vmin}{2*Vn} \tag{1}$$

Total Harmonic Distortion (THD): is "the root mean square ratio of the harmonic content, considering harmonic components up to the 50th order and specifically excluding

*E-mail address: mzamboti@id.uff.br
ISSN: 1791-2377
doi:10.25103/jestr.161.24

interharmonics, expressed as 1% (one percent) of the fundamental. Harmonic components of orders greater than 50th may be included when necessary." [5,6]. It provides the heating potential resulting from distortions generated by harmonics (V_h or I_h) in relation to the fundamental (V_1 or I_1), given in relation to voltage (Eq. 2) or current (Eq. 3).

$$THD_V = \frac{\sqrt{\sum_{h=2}^{\infty}(Vh)^2}}{V_1} = \sqrt{\left(\frac{V}{V_1}\right)^2 - 1} = \sqrt{\frac{V^2 - V_1^2}{V_1^2}} = \frac{V_h}{V_1} \quad (2)$$

$$THD_I = \frac{\sqrt{\sum_{h=2}^{\infty}(Ih)^2}}{I_1} = \sqrt{\left(\frac{I}{I_1}\right)^2 - 1} = \sqrt{\frac{I^2 - I_1^2}{I_1^2}} = \frac{I_h}{I_1} \quad (3)$$

Where V and I are the total voltages and currents that consider the harmonic components (V_h or I_h) injected or added into the fundamental components (V_1 or I_1), respectively [7].

Total Demand Distortion (TDD): according to [5,6], the Total Demand Distortion (TDD) can be defined as "the proportion of the root mean square of the harmonic content, considering harmonic components up to the 50th order and specifically excluding interharmonics, expressed as 1% (one percent) of the maximum demand current. Harmonic components of orders greater than 50th may be included when necessary." Compares the measured harmonics in relation to the total (maximum) demand current of the load (I_L), as postulated in Eq. 4.

$$\mathrm{TDD} = \mathrm{TDD_I} = \frac{\sqrt{\sum_{h=2}^{\infty}(\mathrm{Ih})^2}}{I_L} = \frac{DHT_I * \mathrm{I1}}{I_L} = \sqrt{\frac{I^2 - I_1^2}{I_L^2}} = \frac{I_h}{I_L} \quad (4)$$

Displacement Power Factor (PF_d): The ratio between the active power (Pm) and the fundamental apparent power (S_{1rms}), can never be greater than unity ($PF_d \leq 1$) [9,10], with the upper limit calculated according to Eq. 5.

$$\mathrm{PFd} = \mathrm{PF} = \frac{\mathrm{Pm}}{\mathrm{S1rms}} = \frac{\mathrm{W}}{\mathrm{VA}} = \cos\varphi \leq 1 \quad (5)$$

Harmonic Power Factor (PF_h): if there is current or voltage harmonic distortion, its value is always higher in relation to the PFt ($1 \geq PFh > PF_t$) [9,10], which can be calculated according to Eq. 6.

$$\mathrm{PFh} = \frac{1}{\sqrt{1+(\mathrm{THD_V})^2}} * \frac{1}{\sqrt{1+(\mathrm{THD_I})^2}}, \quad (6)$$

if there is THD_V and THD_I

True Power Factor (PF_t): in nonlinear situations, where the signals are not sinusoidal, the displacement angle (α_d) is different from 0º (zero degrees), so PF_t (or cos φ_t) will be different from the displacement power factor (cos φ or cos φ_d), able, according to [9,10], which can be calculated according to Eq. 7.

$$\mathrm{PFt} = \left(\frac{\mathrm{Pm}}{\mathrm{S1rms}}\right) * \left(\frac{1}{\sqrt{1+(\mathrm{THD_V})^2}}\right) * \left(\frac{1}{\sqrt{1+(\mathrm{THD_I})^2}}\right) \quad (7)$$

Harmonic Pollution (HP): is the total contribution of all harmonic components generated by nonlinear loads and injected into the electrical network or circuit. Its calculation considers both the voltage total harmonic distortion (THD_V) and the current Total Harmonic Distortion (THD_I) [11], according to Eq.8.

$$\mathrm{HP} = \sqrt{(\mathrm{THD_V})^2 + (\mathrm{THD_I})^2} \quad (8)$$

2.1 Characteristics of Shunt Active Power Filters (SAPF)

These types of filters are capable of mitigating most disturbances that contribute to the increase in reactive power, unbalanced currents, harmonics, and electrical fluctuations in voltage and/or current [11,12], as well as for reducing power factors (displacement, distorted or true) resulting from nonlinear loads coupled to the Electrical Power System (EPS), The main function of the SAPF is to mitigate the total current distortion (THD_I), through the compensation current (I_C) injected into each phase of the PCC, aiming to cancel the harmonics generated. by the nonlinear loads and that, perhaps, can be conducted to the generation system or to the source of the EPS [11,12,13,14]. The Fig. 1 presents the working principle of the SAPF, which is based on the IRP theory to generate the filtered compensated currents (filtered I_C or I_{Cabc}), also known as the three-phase compensated currents of said filter.

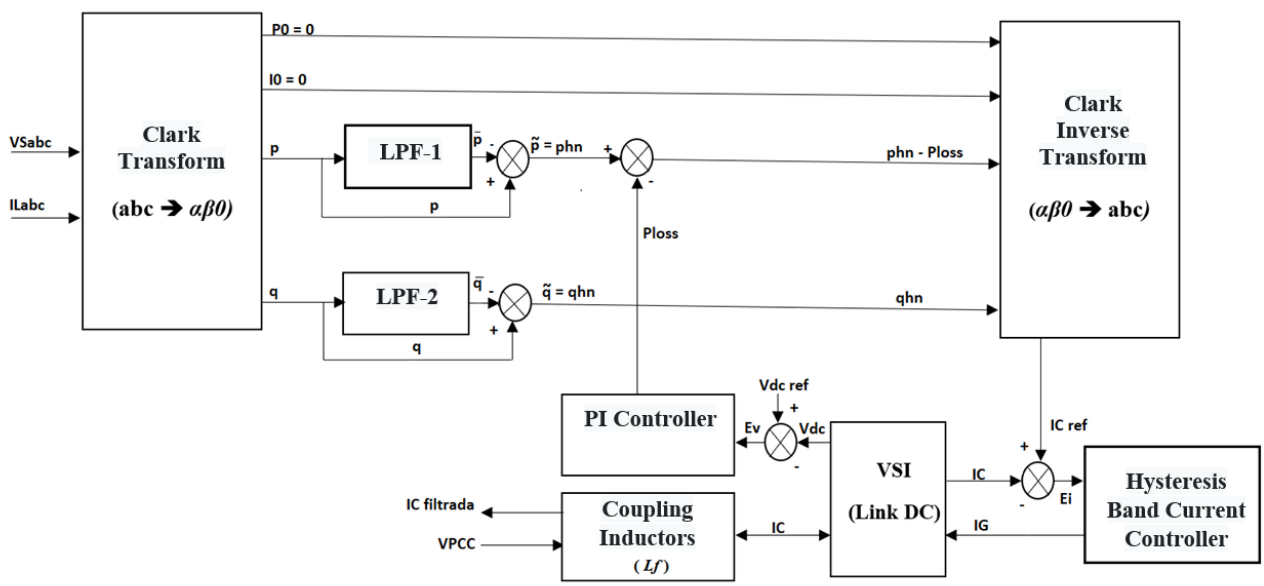

Fig. 1. Block diagram containing an SAPF with its main systems

The design of a Shunt Active Power Filter (SAPF) is composed of five main circuits [15,16.17.18,19,20,21,22,23], as shown in Fig. 1. The first circuit is a Voltage Source Inverter (VSI) responsible for generating compensated currents (IC or ICabc) and the direct current voltage (V_{DC}) [14,15,16]. The second circuit contains three coupling inductors (Lf) that couple and decouple the SAPF from the Power System and filter the residual harmonics of the compensated currents [14,17,18,19]. The third circuit includes a Proportional-Integral (PI) controller that keeps the voltage in the capacitor constant and generates the power (Ploss) needed to compensate for the losses caused by the VSI switching [14,20.21.22,23,24,25,26]. The fourth circuit is a combined set of circuits (Low Pass Filters and comparators) and algorithms (Clarke Transform and Inverse Clarke Transform) that calculates the instantaneous powers and reference compensated currents and eliminates the oscillatory and continuous parts 14,22,23]. Finally, the fifth circuit is called Hysteresis Band Current Controller (HBCC) which is responsible for generating the pulsed currents (IGabc) sent to the VSI to switch the gates of the six Metal Oxide Semiconductor Field Effect Transistors (MOSFETs) that compose the VSI [27,28,29,30,31].

2.2 Procedure for generating the reference compensated currents ($I_{Cabc\ ref}$)

In order to generate the reference compensated currents, two changes of coordinates are necessary (from *abc* to $0\alpha\beta$ and from $0\alpha\beta$ to *abc*), the first uses the Clarke Transform to change the *abc* (120º lag between the voltage or current phases) for $0\alpha\beta$ (90º lag between voltage or current phases), in this step, in addition to calculating the instantaneous powers of zero sequence (P_0), active (p) and reactive (q), the value of the current of zero sequence (I_0). In the second stage of the transformation, the Inverse Clarke Transform is used to return to the origin coordinates (*abc*) and, with this, find the values of the reference compensated currents in these coordinates (I_{Cabc}) [10,14,32,33]. In Eq. 9 to 12, the aforementioned transformations are shown, such that:

Clarke transform: through this transformation, the voltages ($V_{0\alpha\beta}$), currents ($I_{0\alpha\beta}$) and powers ($p_{0\alpha\beta}$) instantaneous in the coordinates) are found $0\alpha\beta$, being:

$$\begin{pmatrix} V_0 \\ V_\alpha \\ V_\beta \end{pmatrix} = \sqrt{\frac{2}{3}} * \begin{vmatrix} \frac{1}{\sqrt{2}} & \frac{1}{\sqrt{2}} & \frac{1}{\sqrt{2}} \\ 1 & -\frac{1}{2} & -\frac{1}{2} \\ 0 & \frac{\sqrt{3}}{2} & -\frac{\sqrt{3}}{2} \end{vmatrix} * \begin{vmatrix} V_{Sa} \\ V_{Sb} \\ V_{Sc} \end{vmatrix} \tag{9}$$

$$\begin{pmatrix} I_{L0} \\ I_{L\alpha} \\ I_{L\beta} \end{pmatrix} = \sqrt{\frac{2}{3}} * \begin{vmatrix} \frac{1}{\sqrt{2}} & \frac{1}{\sqrt{2}} & \frac{1}{\sqrt{2}} \\ 1 & -\frac{1}{2} & -\frac{1}{2} \\ 0 & \frac{\sqrt{3}}{2} & -\frac{\sqrt{3}}{2} \end{vmatrix} * \begin{vmatrix} I_{La} \\ I_{Lb} \\ I_{Lc} \end{vmatrix} \tag{10}$$

$$\begin{pmatrix} p_0 \\ p_\alpha \\ p_\beta \end{pmatrix} = \begin{vmatrix} V_0 & 0 & 0 \\ 0 & V_\alpha & V_\beta \\ 0 & V_\beta & -V_\alpha \end{vmatrix} * \begin{vmatrix} I_{L0} \\ I_{L\alpha} \\ I_{L\beta} \end{vmatrix} \tag{11}$$

Inverse Clarke Transform: by means of this transformation, the reference compensated currents are found ($I_{Cabc\,ref}$) from the SAPF in the coordinates *abc*, where:

$$\begin{pmatrix} Ic_{a\,ref} \\ Ic_{b\,ref} \\ Ic_{c\,ref} \end{pmatrix} = \sqrt{\frac{2}{3}} * \begin{vmatrix} \frac{1}{\sqrt{2}} & 1 & 0 \\ \frac{1}{\sqrt{2}} & -\frac{1}{2} & \frac{\sqrt{3}}{2} \\ \frac{1}{\sqrt{2}} & -\frac{1}{2} & -\frac{\sqrt{3}}{2} \end{vmatrix} * \begin{vmatrix} I_{L0} \\ I_{L\alpha} \\ I_{L\beta} \end{vmatrix} \tag{12}$$

3. Methodology and Modeling

The simulation was divided into two stages, where in the first stage, the APF was considered off (without compensation), while in the second stage the said filter was inserted into the ship's electrical system in order to compensate for the unwanted harmonics conducted by the nonlinear loads (C_1 and C_2) connected to the Point of PCC. Aiming to measure the harmonics conducted by the mentioned nonlinear loads, in the first stage of the simulation, the loads were connected to the EPS as follows: (I) C_1, C2, and C3; (II) C_1 and C_3; and (III) C_2 and C_3. Based on these configurations, the EPS was loaded at 85.61% (C_1, C_2, and C_3), 17.58% (C_1 and C_3), and 81.31% (C_2 and C_3), respectively.

For a better understanding and visualization of the proposed model, Figure 2 presents the Electric Power Generation and Distribution Systems (EPGDS) of the CCB, containing only the Consumer Units (C or CU, from 1 to 3) that will be simulated together with the Genset (G_S).

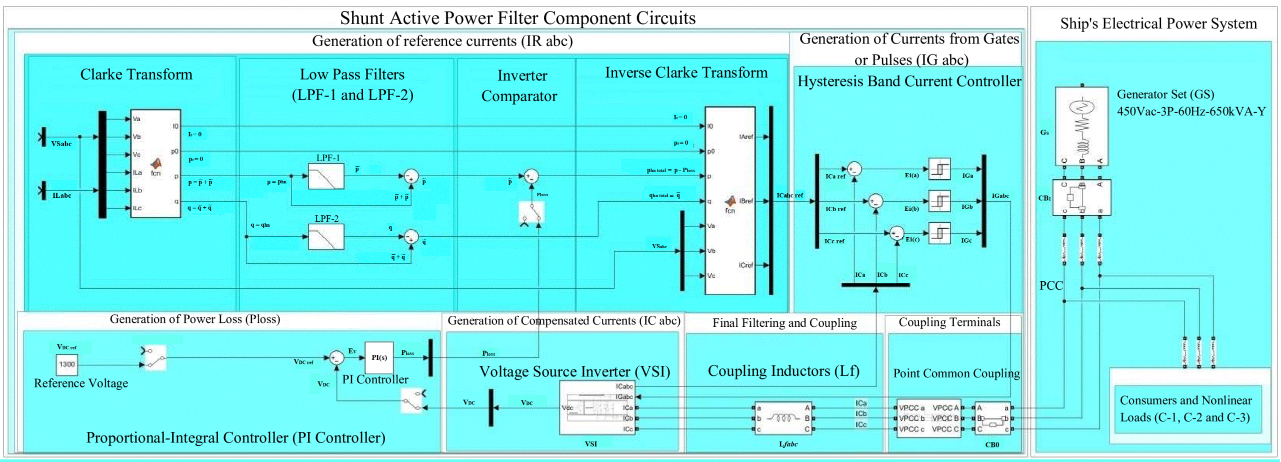

Fig. 2. Partial Modeling of Generation and Distribution Systems, containing only the most critical Users to be simulated together with the designed SAPF

3.1 Partial lifting of the loads

In Tab. 1, the maximum capacities of the electrical quantities of the equipment to be modeled are presented, such as: apparent power (S_{Lmax}); effective line voltage (V_{Lmax}); effective line current (I_{Lmax}); true power factor (PF_t); Line impedance (Z_L); short-circuit ratio (R_{SC}); and short-circuit current (I_{SC}).

Table 1. Capabilities of the Ship Equipment to be Simulated and Modeled.

Equipment	Description	S_{Lmax} (kVA)	V_{Lmax} (V)	I_{Lmax} (A)	PF_t (pu)	Z_L (Ω)	R_{SC} (pu)	I_{SC} (A)
G_S	Genset	650	450	834	0.80	0.54	≤ 20	16,680
C1 or CU-1	24 V_{DC} rectifiers	16	440	20	1	12.7	≤ 20	400
C2 or CU-2	* MLS and specific equipment	550	440	721	0.8	0.35	≤ 20	14,434
C3 or CU-3	Three-phase Induction Motor (TIM)	105	440	138	0.86	1.84	≤ 20	2,760
SAPF	Shunt Active Power Filter	170	440	225	0.98	1.13	≤ 20	4,500

* MLS: Main Lighting System and specific equipment (radars, sensors, weapons, inverters, and computers) installed on the Ship under study.

3.2 Limits of some electrical parameters established in standards

After the two simulation stages of the proposed model, the results that were found were compared with the standardized limits [4,5,6] and presented in Tab. 2 in order to evaluate the parameters that were measured before and after the implementation of SAPF.

Table 2. Ship Power System Voltage and Current Harmonic Distortion Limits.

$V_{PCC} \leq 1$ kV (THD) and 120 V ≤ $V_{PCC} \leq 69$ kV (TDD)							
$R_{SC} \leq 20$ (pu)	PF_{tEPS} (pu)	VM_{EPS} (%)	HP_{EPS} (%)	h_{EPS} (pu)	THD_{VEPS} (%)	THD_{VEPS} (%)	TDD_{IEPS} (%)
20	≥ 0.80	≤ 2.00	≤ 7.00	1 < h ≤ 50	5.00 [4]	8.00 [5]	5.00

4. Simulations and Results

As the Three-phase Induction Motor (TIM) of the Water Cooling Unit (WCU or C_3) does not generate significant harmonics with respect to the nonlinear loads (C_2 and C_3), in order to verify the harmonic distortions conducted to the distribution system through the PCC, the system loading was performed according to the following load configurations: I (C_1, C_2 and C_3), II (C_1 and C_3) and III (C_2 and C_3), as can be seen in Fig. 3, Fig. 4, and Fig. 5.

As can be seen in Fig. 3, when connecting the loads C_1, C_2, and C_3 to the PCC, the EPS was loaded at 85.61% (546.46 kVA) of its maximum demand (650 kVA). Under these conditions, a PFt value of 0.74 was measured.

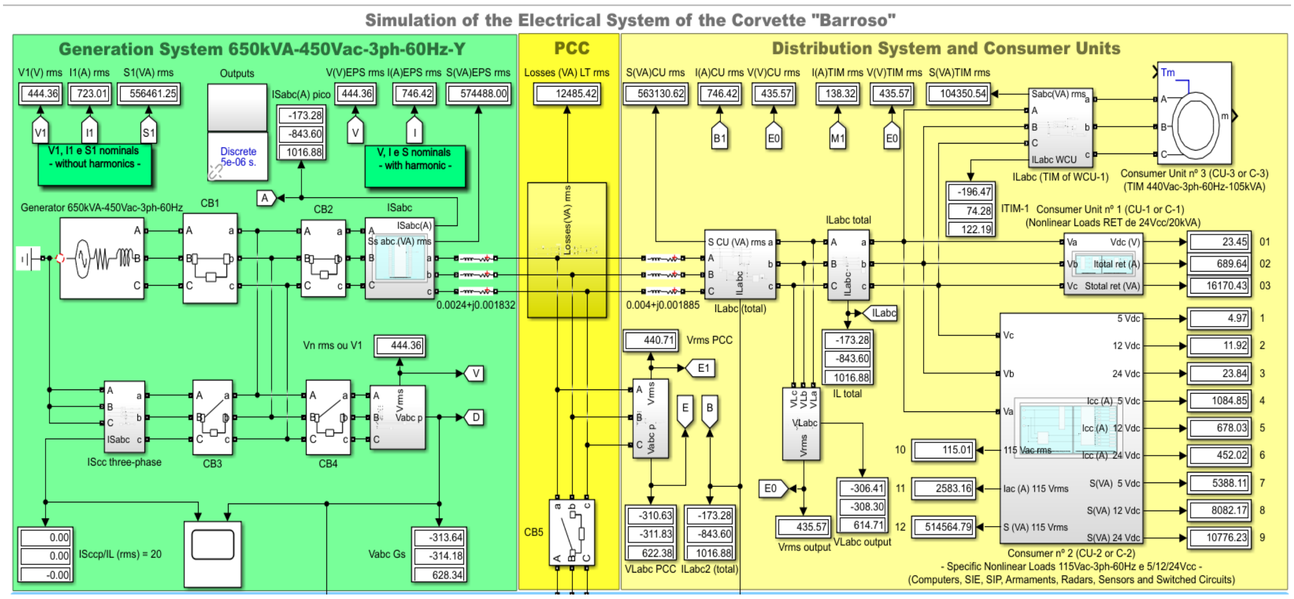

Fig. 3. Simulation with the ship's EPS loaded in the configuration I (C_1, C_2, and C_3)

After loading the EPS following configuration II, as shown in Fig. 4, the measured value of FPt_{SEP} was equal to 0.80 for a demand of 17.60% or 114.25 kVA (C1 and C3 connected to the PCC).

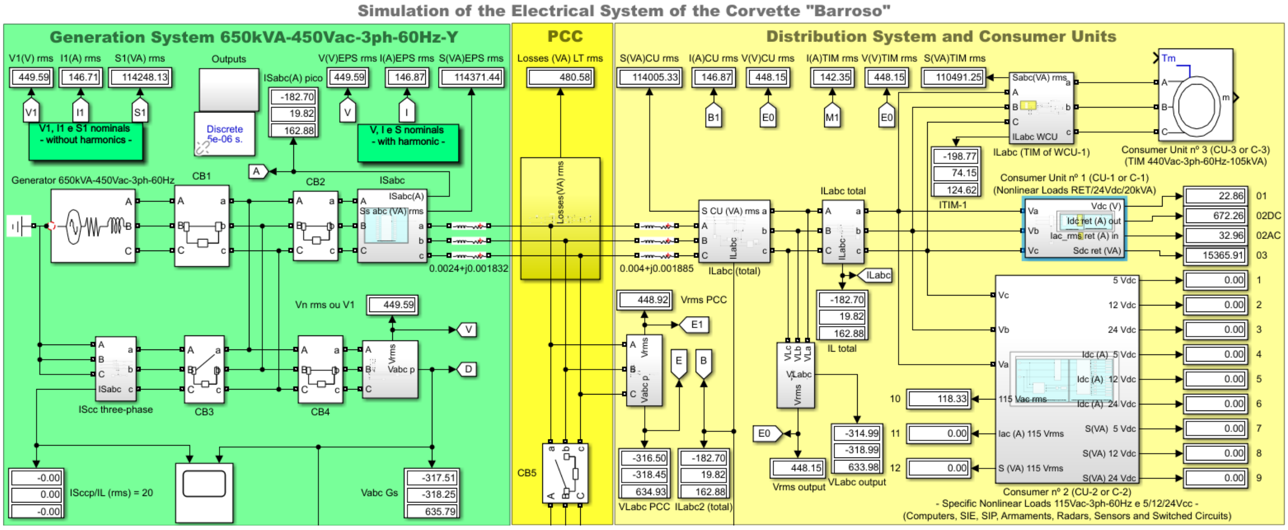

Fig. 4. Simulation with the ship's EPS loaded in the configuration II (C_1 and C_3)

When loading the EPS according to Fig. 5 (configuration III), the demanded power of the system was around 81.31% of the maximum demand (650 kVA) and the measured $FP_{t\ EPS}$ was 0.73.

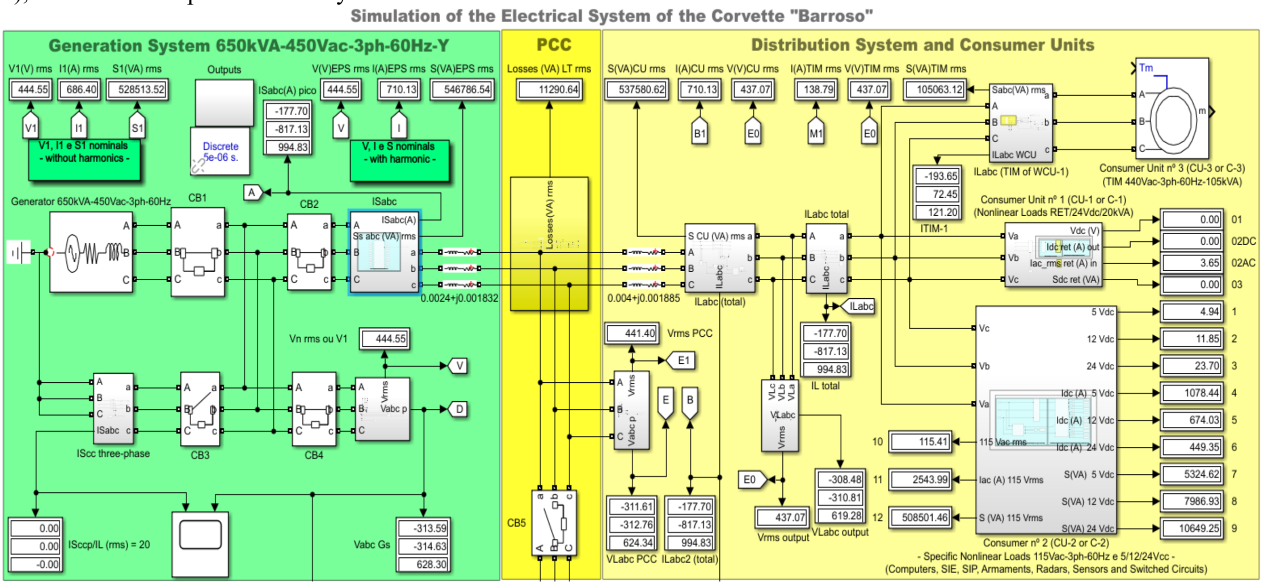

Fig. 5. Simulation with the ship's EPS loaded in the configuration III (C2 and C3)

4.1 Analysis of the results found in the first stage of the simulation (SAPF off)

The results found were based on each loading configuration (I, II, or III) of the EPS with the SAPF turned off, and therefore each condition was performed separately.

4.1.1 Analysis of the results found in configuration I and SAPF turned off

As can be seen in Fig. 6, practically all voltage (VLabc) and current (ILabc) harmonic distortions and deformations, generated by the CU (on the left side of the figure) coupled to the PCC, were conducted to the output terminals of the generator set, which causes considerable deformations in the shapes of voltage (VSabc) and current (ISabc) waveforms at the output of the mentioned generator.

According to Fig. 7, the total voltage and current harmonic distortions generated by the Consumers (CU-1, CU-2 and CU-3) were around 1.33% ($THD_{V\ CU}$) and 25.58% ($THD_{I\ CU}$), respectively. Therefore, although the $THD_{V\ CU}$ (1.33%) was within the limits established in the norms ($THD_{V\ norm} \leq 5\%$ or 8%), the value found for the $THD_{I\ CU}$ (25.58%) is in disagreement with relation to the current norms [4,5] ($THD_{I\ CU\ norm} \leq 5\%$) and as in the first stage of the simulation the SAPF is turned off, most of these distortions were conducted to the EPS of the Ship.

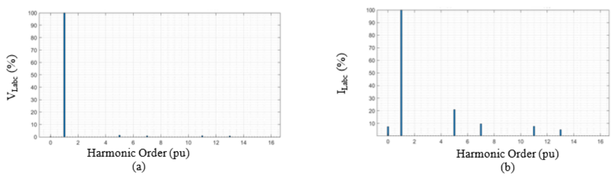

Fig. 7. Voltage (a) and current (b) harmonic components generated in configuration I

In Fig. 8 shows the values of $THD_{V\ EPS}$ (0.36%) and $THD_{I\ EPS}$ (25.58%), measured from the output terminals of the G_S, respectively. It can be verified that, although the $THD_{V\ EPS}$ (0.36%) was within the limits established in norms ($THD_{V\ norm} \leq 5\%$ or 8%), the $THD_{I\ EPS}$ (25.58%) was also outside of the limits standardized ($THD_{V\ norm} \leq 5\%$).

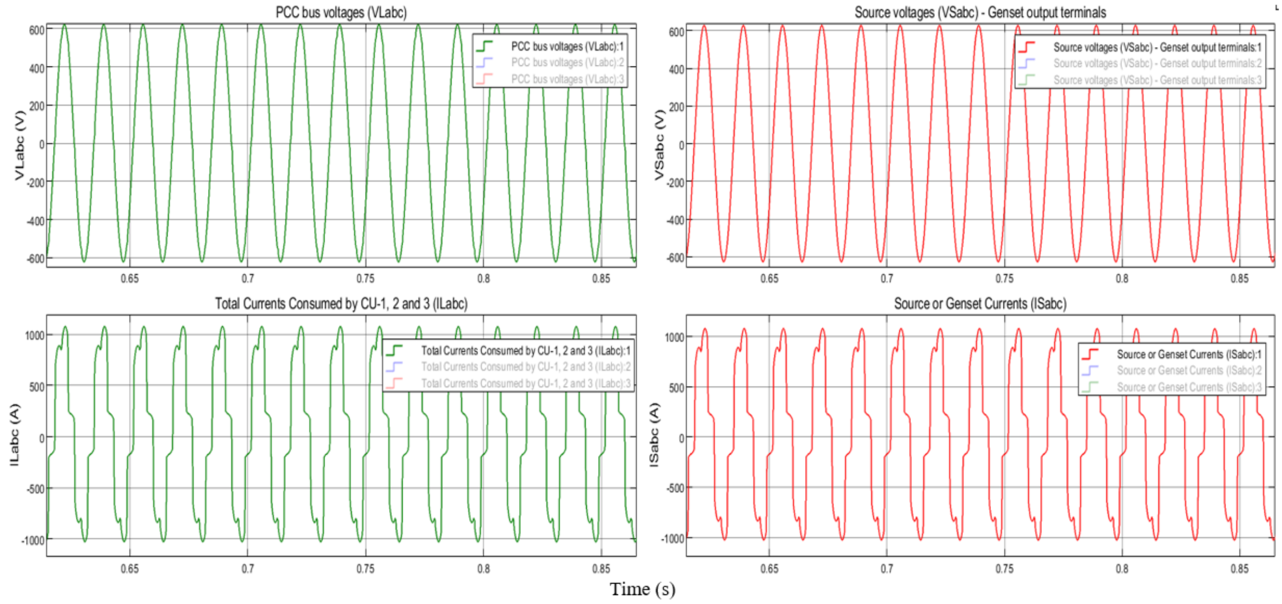

Fig. 6. Voltage and current waveforms at the load (green) and genset (red) terminals in the configuration I

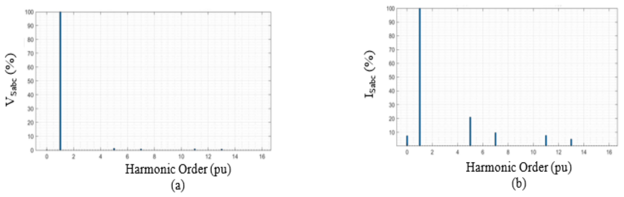

Fig. 8. Voltage (a) and current (b) harmonic components conducted to the EPS in the configuration I

4.1.2 Analysis of the results found in configuration II and SAPF turned off

According to Fig. 9, the nonlinear load (C_1) was not able to cause a relevant deformation in the equivalent waveform measured at the PCC, indicating that configuration II (C_1 and C_3) did not cause changes outside the standardized patterns or that justify the activation of SAPF when the ship is operating under these load conditions.

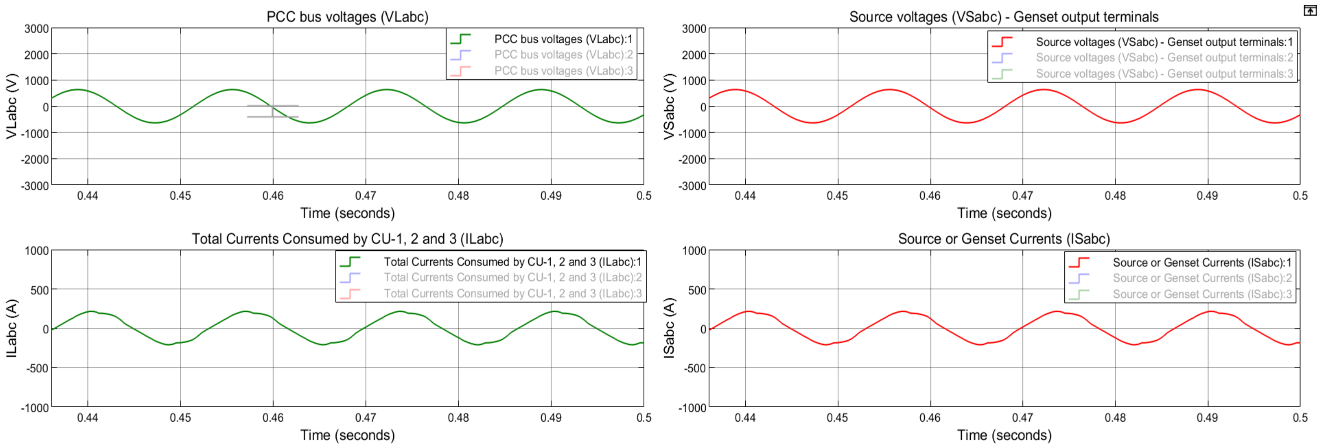

Fig. 9. Voltage and current waveforms at the load (green) and genset (red) terminals in configuration II

The Fig 10 (charts from “a” to “d”) show the THD generated by the loads (Fig. 10a and Fig. 10c) and conducted to the output terminals of the genset (Fig. 10b and Fig. 10d), indicating the voltage and current distortions of the CUs (THD_{VCU}=0.02% and THD_{ICU}=3.76%) and the EPS (THD_{VEPS}=0.02% and THD_{IEPS}=1.59%), respectively. It can be observed that all values related to THD remained below 5% and therefore in compliance with the limits recommended by the current standards (Tab. 2).

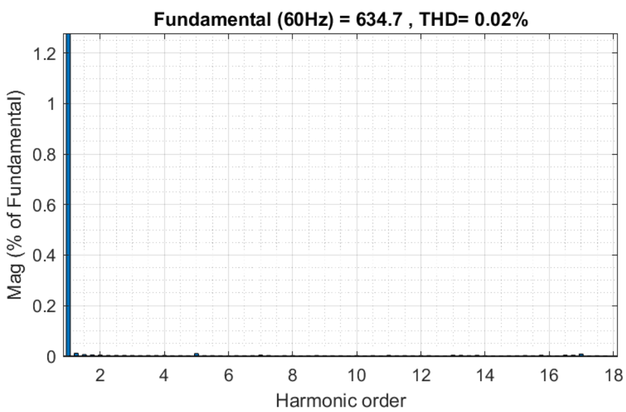

a)$THD_{V\,(CU)}$ with C_1 and C_3 coupled to the EPS

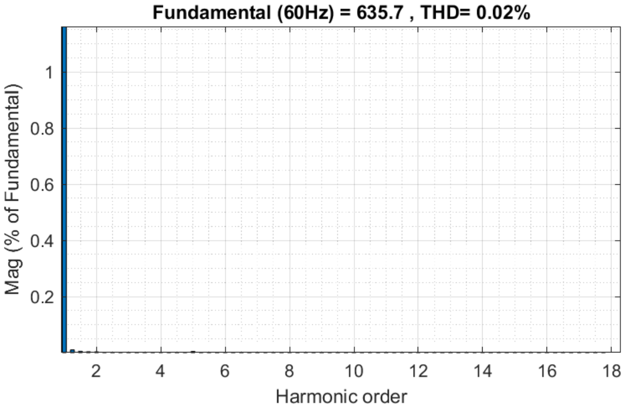

b) $THD_{V\,(EPS)}$ with C_1 and C_3 coupled to the EPS

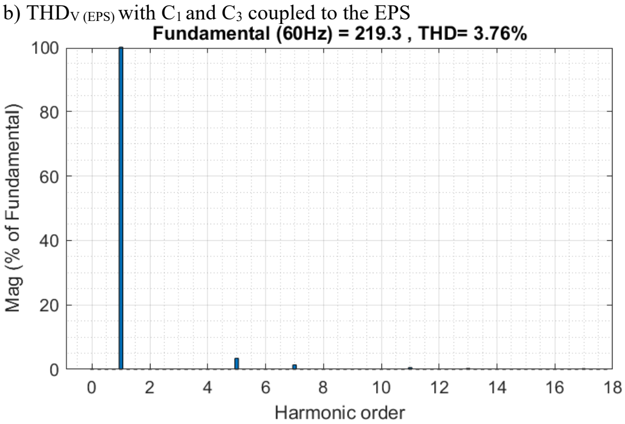

c) $THD_{I\,(CU)}$ with C_1 and C_3 coupled to the EPS

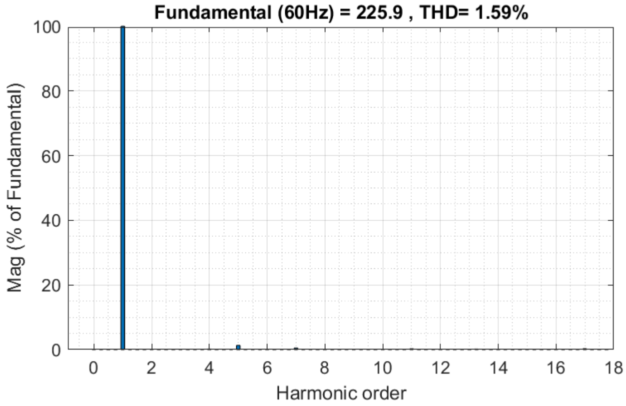

d) $THD_{V\,(EPS)}$ with C_1 and C_3 coupled to the EPS

Fig. 10. THD of voltage and current conducted to the EPS in configuration II

4.1.3 Analysis of the results found in configuration III and SAPF turned off

Unlike configuration II, Fig. 11 shows that, when the system was operated in configuration III, despite the voltage waveforms not suffering considerable distortions, the harmonics conducted to the EPS in this configuration were able to significantly deform the current waveform (ISabc) of the system (graph indicated in red). This distortion is justified due to the non-linear load C_2 (computers, radars, weapons systems, among others), since, as verified in configuration II, C_3 did not cause deviations outside the standards established by regulations, even when operating together with non-linear loads represented by the 24Vdc rectifiers (C_1).

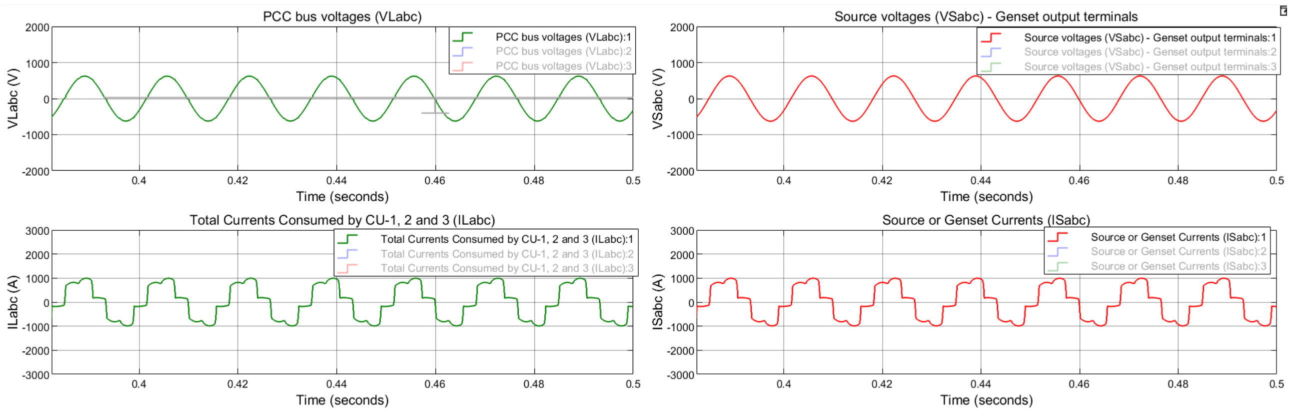

Fig. 11. Voltage and current waveforms at the load (green) and genset (red) terminals in configuration III

Through the graphs from a) to d) shown in Fig.12, it can be verified that the voltage harmonics generated by users in configuration III (1.33%) were not sufficient to cause a DHT_V (0.35%) outside the limits allowed by regulations ($THD_V \leq 5\%$) in the ship's system. However, the current distortions generated by the loads (26.55%) were entirely conducted to the ship's EPS (26.55%), consequently causing a THD outside the acceptable limits expressed in Tab. 2.

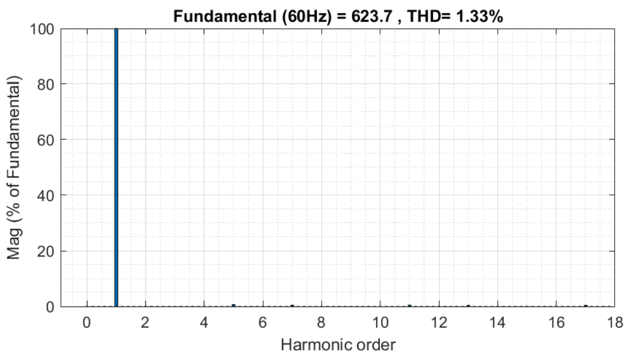

a) $THD_{V\,(CU)}$ with C_2 and C_3 coupled to the EPS

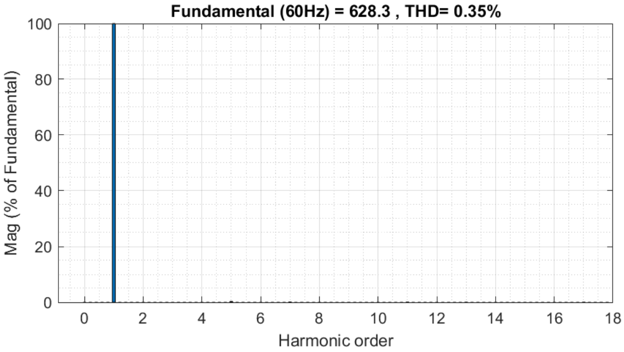

b) $THD_{V\,(EPS)}$ with C_2 and C_3 coupled to the EPS

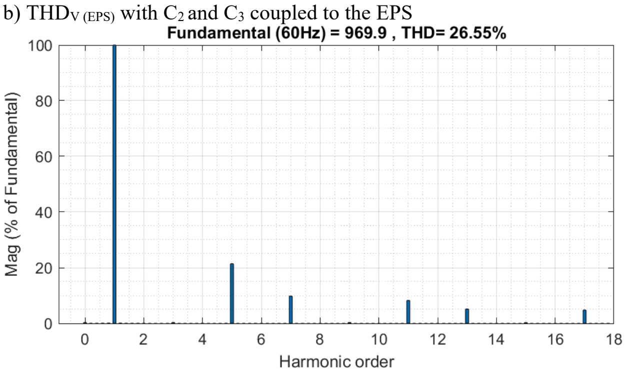

c) $THD_{I\,(CU)}$ with C_2 and C_3 coupled to the EPS

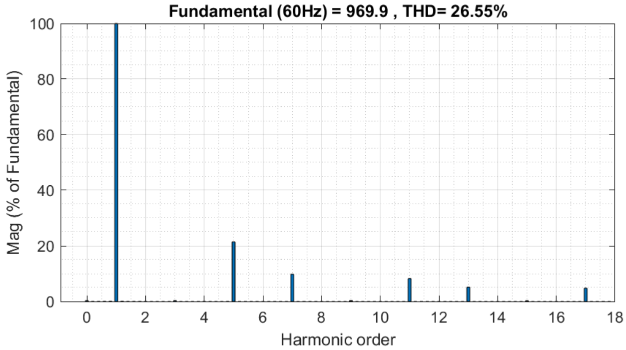

d) $THD_{V\,(EPS)}$ with C_2 and C_3 coupled to the EPS

Fig. 12. THD of voltage and current conducted to the EPS in configuration III

When comparing the values from Tab. 3 with those standardized in Tab. 2, it was found that only configuration II (C_1 and C_3) presented values in conformity with current standards, indicating that the unit causing harmonic distortions in the EPS (outside standardized values) is C_2 or CU-2. Therefore, it is not necessary to test all configurations (I, II, and III) in conjunction with the SAPF. In other words, only configuration I (C_1, C_2, and C_3) is sufficient to ensure and demonstrate the effectiveness of the SAPF suggested in this research. The Tab. 3 presents some results obtained in the first stage of the simulation, considering the three types of configurations (I, II, and III) mentioned above.

Table 3. Results found in the simulation with SAPF turned off.

Loading of the system according to the type of configuration (I, II and III) (%)	THD_V CU (%)	THD_I CU (%)	TDD_I CU (%)	THD_V EPS (%)	THD_I EPS (%)	TDD_I EPS (%)	HP EPS (%)	VM EPS (%)	PF_t EPS (pu)
85.61 (I or C_1, C_2 and C_3)	1.33	25.58	25.58	0.36	25.58	25.58	25.61	0.1300	0.74
17.58 (II or C_1 and C_3)	0.02	3.76	3.76	0.02	1.59	1.59	1.59	0.002	0.80
81.31 (III or C_2 and C_3)	1.33	26.55	25.55	0.35	26.55	25.66	0.44	0.008	0.73

4.2 Simulation with SAPF turned on

As already mentioned in the first stage of the simulation, the most relevant load in relation to the generation of harmonics outside the limits established in the standard was C2, therefore, it is not necessary to simulate all three configurations, that is, to validate the SAPF, it is enough to simulate the worst situation with respect to harmonic distortions that, in this case, configuration I is the most adequate and, therefore, chosen to meet the purpose of this study.

4.2.1 SAPF parameters used in the simulation

In Tab. 4, are presented the main parameters of the SAPF used in the second stage of the simulation. Details on the design, calculation, and dimensioning of the SAPF can be consulted at [10,14,15,14,32,33]. Bearing in mind that, in most cases, the SAPF are applied with the purpose of mitigating the harmonic current distortions carried to the source by the nonlinear loads coupled to the PCC of the EPS and, with this, improving, mainly, the following parameters: PF_V, HP, THD_I, TDD_I, reactive power and the waveform of the currents distortions [4,5,6,10,14,19,20,22,33].

Table 4. Specifications of the electrical parameters of the SAPF used in the simulation.

PI Controller		VSI		Inductors of Coupling		Low Pass Filters (LPF-1 and LPF-2)		Controller (HBCC) *	
G_P (pu)	8	V_{DC} (V)	1,300±5%	L_f (µH)	70±8%	f_{c1} and f_{c2} (Hz)	70±0.5%	G_H Hysteresis (pu)	1.27
G_I (pus)	8,000	$I_{max\ head}$ (A)rms	225	V_{max} (V)rms	600	C_1 and C_2 (mF)	10±0.5%	$I_{Cabc\ ref\ max}$ (A)peak	500
T_I (ms)	1	f_{SW} (kHz)	10	I_{Cabc} (A)rms	225±5%	F_{an} and F_{a2} (pu)	44	$Im_{ax\ head}$ (A)peak	540
Ploss (kW)	52	h (pu)	19	V_{PCC} (V)rms	440±5%	R_1 and R_2 (Ω)	1±0.5%	LB (A)peak	±50.8
V_{DCref} (V)	1,300	C_{DC} (µF)	1,000±8%	-	-	τ (s)	10	Mistake (A)peak	50.8

* HBCC: Hysteresis Band Current Controller

4.2.2 Simulated system in the configuration 1 (C_1, C_2, and C_3 coupled to EPS with the SAPF turned on)

The Fig. 13 presents the second stage of the simulation, in which the Ship's EPS was loaded with all loads (C_1, C_2, and C_3) and put into operation together with the SAPF.

The Tab. 5 shows the parameters measured during the simulation with the SAPF turned. Analyzing the results found it is verified that all the values of the electrical parameters of the EPS ($THD_{I\ EPS}$, $TDD_{I\ EPS}$, HP_{EPS}, VM_{EPS} and $PF_{V\ EPS}$) were within of the normalized limits (Tab. 2). It is worth mentioning that the SAPF is not implemented to mitigate the harmonics resulting from the CUs, but, through the injection of harmonics in the PCC, to prevent the harmonics generated by these loads from being conducted to the EPS, this explains the reason why the value of $THD_{I\ CU}$ (26.33%) has remained outside the limits provided by Tab. 2, even considering the SAPF performance in the Ship's EPS.

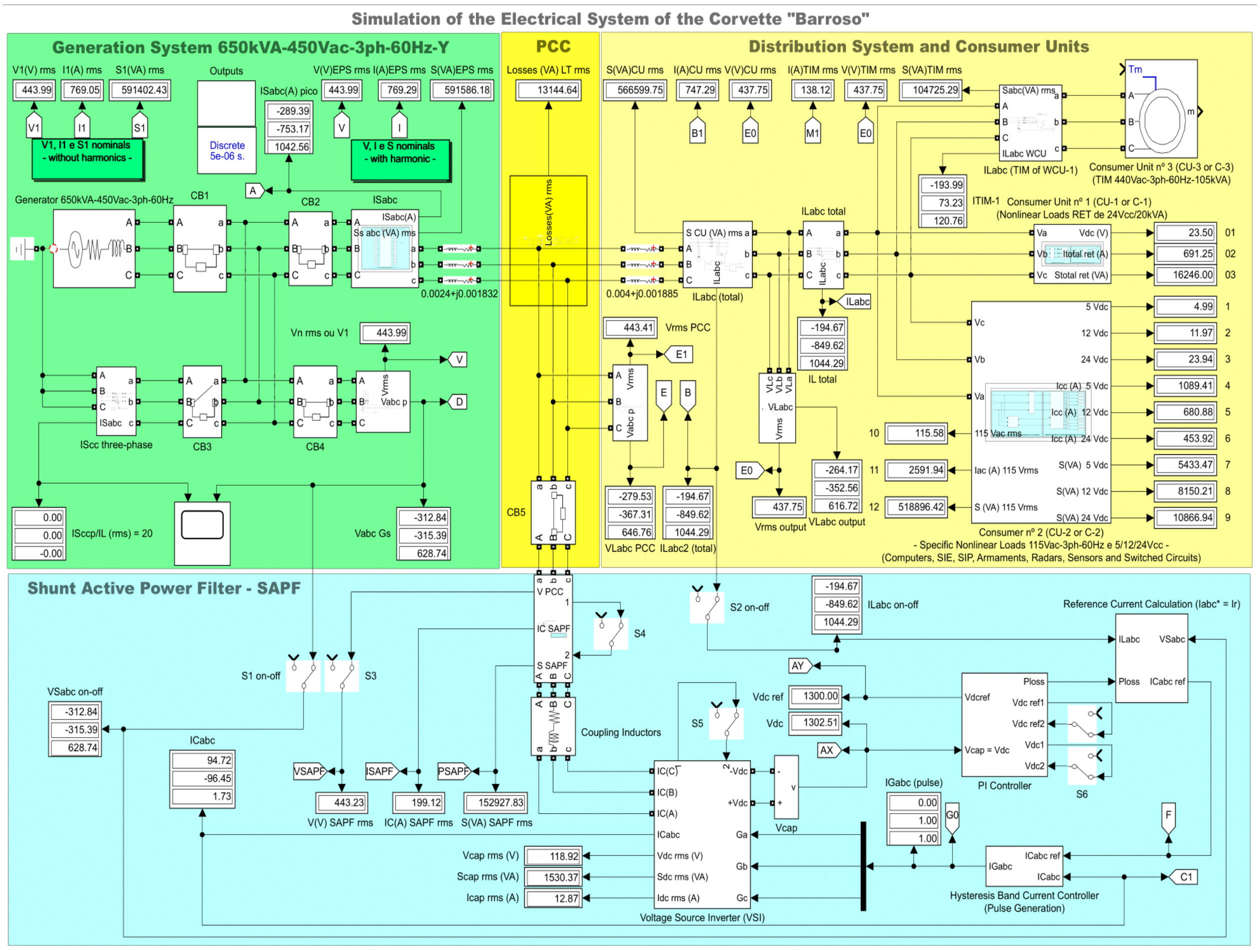

Fig. 13. Modeling and simulation with the Ship's EPS loaded

Table 5. Results found in the simulation with SAPF turned on.

Loading and system configuration (CU and %)	THD_V CU (%)	THD_I CU (%)	TDD_I CU (%)	THD_V EPS (%)	THD_I EPS (%)	TDD_I EPS (%)	HP EPS (%)	VM EPS (%)	PF_t EPS (pu)
C_1, $C_{2/}$ and C_3 (85.61)	0.03	26.33	26.33	0.02	0.50	0.50	0.50	0.013	0.97

Analyzing the Fig. 14, it is possible to observe that the SAPF implemented in the simulation managed to considerably attenuate the harmonic distortions of the EPS, producing voltage and current waveforms very close to a perfect sinusoid.

As the SAPF injects current harmonics into the CUs, aiming to compensate the harmonics generated by these loads and, with this, preventing them from being conducted to the EPS or to the main power supply of the Ship, there was a small increase in total current harmonic distortions. of loads ($THD_{I\ CU}$), that is, increasing from 25.58% to 26.33%. However, the $THD_{V\ CU}$ decreased from 1.33% to 0.03%, and their respective graphs are represented in Fig. 15.

As per Fig. 16, it can be seen that the SAPF considerably mitigated $THD_{V\ EPS}$ (from 0.36% to 0.02%), $THD_{I\ EPS}$ (from 25.58% to 0.50%) and $TDD_{I\ EPS}$ (from 25.58% to 0.51%). Thus, both results are in accordance with the standardized limits ($THD_{V\ EPS}$, $THD_{I\ EPS}$ and $TDD_{I\ EPS}$ less than 5%).

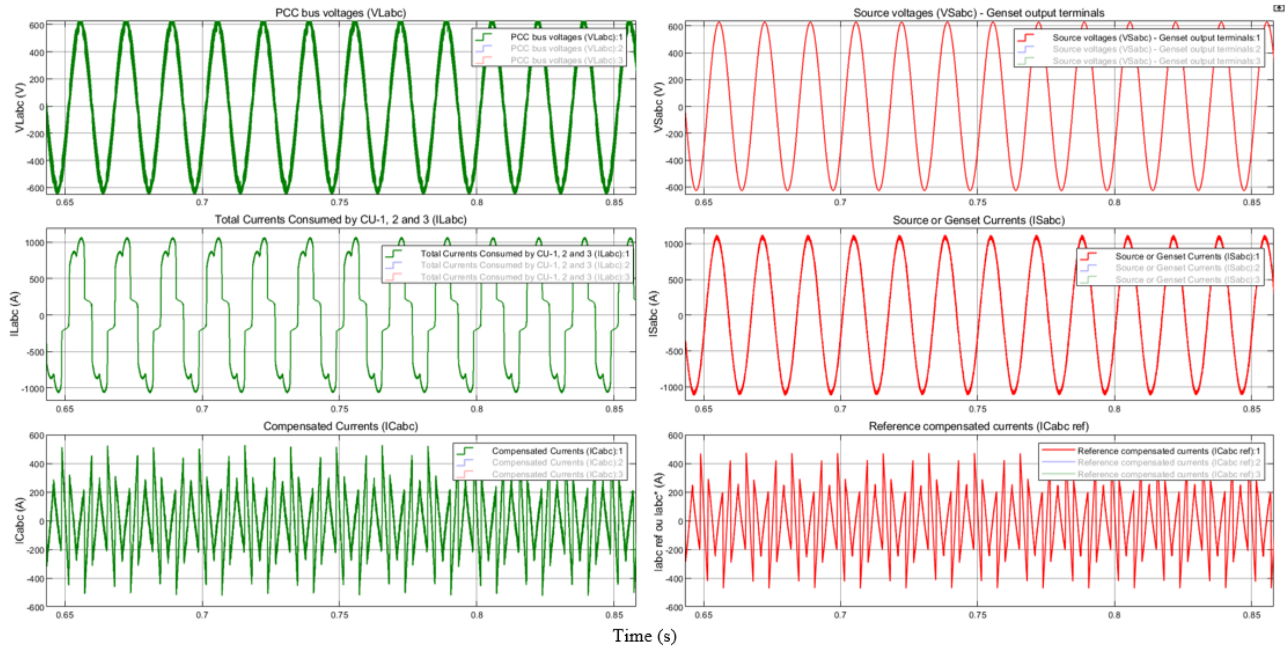

(a) (b)

Fig. 14. Voltage and current waveforms at the load (a) and generator (b) terminals with SAPF in operation and the system loaded at 85.61% of its maximum capacity.

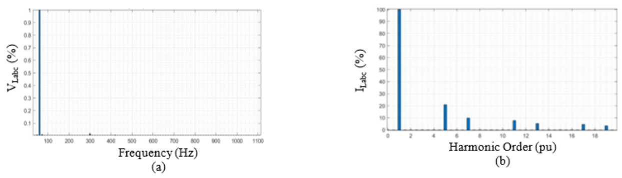

Fig. 15. Voltage (a) and current (b) harmonic components generated by nonlinear loads with SAPF acting

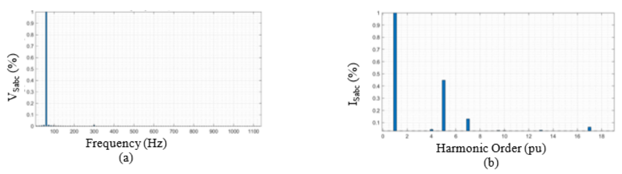

Fig. 16. Voltage (a) and current (b) harmonic components conducted to the genset output terminals with SAPF acting

5. Conclusions

The simulation was divided into two stages, where in the first stage the SAPF was turned off, while in the second stage the said filter was connected to the ship's EPS. In order to verify which of the loads (C_1, C_2, or C_3) conducted more harmonics to the Ship's EPS, only the first stage of the simulation was divided into three distinct load configurations (I-C_1, C_2, and C_3, II-C_1 and C_3, and III-C_2 and C_3), where it was proven that configuration I was the most significant in this regard and, therefore, chosen to be analyzed in the second stage of the simulation.

Through this research, it was possible to prove that the SAPF implemented in the vessel's system was able to significantly compensate the harmonics generated by non-linear loads, that is, the parameters were within the limits established at current standards ($THD_{V\ EPS} = 0.03\%$, $THD_{I\ EPS} = 0.50\%$, and $TDD_{I\ EPS} = 0.51\%$, both less than 5%), resulting in a reduction of the Harmonic Pollution of the EPS (HPEPS), from 25.58% to 0.005% (below 7%, value established in the standard). After the inclusion of SAPF in the simulation, other important factors were also improved, they were, the true power factor and the voltage modulation, presenting values equal to 0.97 ($PF_{t\ EPS} \geq 0.80$) and 0.013% ($VM_{\ EPS} \leq 2\%$), respectively.

In view of the above, the SAPF chosen in this research was able to compensate for the current harmonics generated by the non-linear consumers of the Ship (C_1, C_2, and C_3) and, with that, mitigating the unwanted harmonic components, preventing these components were injected into the main power supply of the CCB, thus increasing the availability of the system and, consequently, contributing to increase the quality of electrical energy of the referred vessel, since all electrical parameters measured during the simulation with the filter acting were in compliance with the standardized values (THD_V, THD_I, and TDD $\leq$ 5%; PFt $\geq$ 0.80; HP $\leq$ 7%; and VM $\leq$ 2%). Thus indicating that the choice of SAPF was adequate and, as a result, was able to contribute satisfactorily to the improvement of the energy quality of the studied ship.

References

1. Freitas, E. S., et al., "A busca da grandeza (VII): retaguardas técnicas". *Revista Matitima Brazileira*, 132, 04 2012, pp. 60-72.
2. Freitas, E. S., et al., "A busca da grandeza (VIII): Marinha e a indústria naval". *Revista Matitima Brazileira*, 132, 07/09, 2012, pp. 39-55.

3. Freitas, E. S., et al., "A busca da grandeza (V): A corveta "Barroso" – primeiro Navio projetado e construído no Brasil republicano. Indispensável o complexo técnico-científico – industrial militar – análise da década de 1980 e início da década de 1990 – o declínio – ciclos de atraso". *Revista Matitima Brazileira*, 131, 07/09, 2011, pp. 9-16.
4. ENGENALMARINST Nº 30-08A. "Especificação das características de Energia Elétrica em Corrente Alternada (CA) e Corrente Contínua (CC) para os utilizadores em Navios de superfície da Marinha do Brasil". *Revista Matitima Brazileira*, 2019, pp. 1-12.
5. IEEE Power and Energy Society. IEEE P519-2014.1/D8B, "D*raft Guide for Applying Harmonic Limits on Power Systems*". USA: Institute of Electrical and Electronics Engineers, 2014, pp. 1-29.
6. IEEE Power and Energy Society. IEEE Std 1159-2009, IEEE "*Recommended Practice for Monitoring Electric Power Quality*". USA: Institute of Electrical and Electronics Engineers, 2009, pp. 1-91.
7. IEEE Power and Energy Society. IEEE Std 1459-2010: "*Standard Definitions for the Measurement of Electric Power Quantities Under Sinusoidal, Nonsinusoidal, Balanced, or Unbalanced Conditions.*" New York, Institute of Electrical and Electronics Engineer, 2010, pp. 1-52.
8. ENGENALMARINST Nº 30-11A. "Especificação de motores de indução e geradores síncronos para uso naval". *Revista Matitima Brazileira*, 2018, pp. 1-28.
9. Grady, W., Gilleskie, R. J., "Harmonics and how they relate to power factor". *In: Proceedings of the EPIR Power Quality Issues & Opportunities Conference*. November, San Diego, CA, 1993, pp. 1-8.
10. Singh, B., Chandra, A., Al-Haddad K., "Power quality: problems and mitigation techniques". John Wiley & Sons, 1ª ed., 2015, pp. 1-600.
11. Biswas, P. P., Suganthan, P. N., Amaratunga, G. A. J., "Minimizing harmonic distortion in power system with optimal design of hybrid active power filter using differential evolution". A*pplied Soft Computing,* UK, 61, 2017, pp. 486-496.
12. Kumar, D. P., et al., "*Investigations on shunt active power filter for power quality improvement*". Master thesis of Technology in Power Control and Drives), National Institute of Technology, Rourkela, 2007, pp. 1-67.
13. Troncha, G. S., et al., "*Uma contribuição à aplicação dos filtros ativos em sistemas elétricos de potência*". Master thesis of the Federal University of Uberlândia, Graduate Program in Electrical Engineering, 2019, pp. 1-157.
14. Unnikrishnan, K. A. E., Chandrika, S. G., Subhash,j. T. S., Manju, A., Joseph, A., "Shunt hybrid active power filter for harmonic mitigation: A practical design approach". *Journal: Sadhana - Academy Proceedings in Engineering Sciences*, Tamil Nadu: Springer, 40, 4, 2015, pp. 1257–1272.
15. Briz, F. et al., "Dynamic behavior of current controllers for selective harmonic compensation in three-phase active power filters". I*EEE Transactions on Industry Applications*, 49, 3, 2013, pp. 1411-1420.
16. Xiongfei, W., Frede, B., Chiang, L. P., "Virtual RC damping of LCL-filtered voltage source converters with extended selective harmonic compensation." IEEE *Transactions on Power Electronics*, 30, 9, 2015, pp. 4726-4737.
17. Venturini, R. P., et. al., "Adaptive selective compensation for variable frequency active power filters in more electrical aircraft". *IEEE Transactions on Aerospace and Electronic Systems*, 48,2, 2012, pp. 1319-1328.
18. A. E. AULD et al., "Load-following active power filter for a solid oxide fuel cell supported load". *Journal of Power Sources*, 195, 7, 2010, pp. 1905-1913.
19. Carpinelli, G., Proto, D., Russo, A., "Optimal planning of active power filters in a distribution system using trade-off/risk method". *IEEE Transactions on Power Delivery*, 32, 2, 2017, pp. 841-851.
20. Shafiuzzaman, K., Malabika, B. Conlon, M. F., "Parallel operation of inverters and active power filters in distributed generation system - A review". *Renewable and Sustainable Energy Reviews*, 15, 9, 2011, pp. 5155-5168.
21. Jou, H. L., Wu, J. C., Chu, H. Y., "New single-phase active power filter". *IEEE Proceedings-Electric Power Applications*, 141, 3, 1994, pp. 129-134.
22. Thomas, T., Haddad, K., Joos, G., Jaafari, A., "Design and performance of active power filters". *IEEE Industry Applications Magazin*e, 4,5, 1998, pp. 38-46.
23. Peng, F. Z., et al., "Application issues of active power filters". *IEEE Industry applications magazine*, 4, 5, 1998, pp. 21-30.
24. Ahmed, A., et al., "*Eletrônica de Potência*". 5ª ed., São Paulo: Prentice-Hall, 2000, p. 480.
25. Wu, B., Narimani, M., "*High-power converters and AC drives*." John Wiley & Sons, 2017, p. 333.
26. Ogata, K., "*Engenharia de controle moderno"*. Brazil: 5ª ed., Pearson, 2010, pp. 1-809.
27. Sabaghi, M., Dashtbayazi, Dashtbayazi, M., Marjani, S., "Dynamic Hysteresis Band Fixed Frequency Current Control". *World*, 2222, 2016, pp. 1-2510.
28. Joos, G., Moran, L., Ziogas, P., "Performance analysis of a PWM inverter VAR compensator." *IEEE Transactions on Power Electronics*, 6, 3, 1991, pp. 380-391.
29. Pomilio, J. A.,"*Fontes chaveadas*" Publicação FEEC, State University of Campinas, Faculty of Electrical and Computer Engineering, Department of Systems and Energy, 13, 2016, pp. 1-95.
30. Kislovski, A., Redl, R., Sakal, N. O.,"*Dynamic analysis of switching-mode DC/DC converters*". 5ª ed., Springer Science & Business Media, 2012, pp. 1-404.
31. Chryssis, G., "H*igh-frequency switching power supplies: theory and design*". McGraw-Hill Companies, 1989. pp. 1-301.
32. Panchbhai, A., Parmar, S., Prajapati, N., "Shunt active filter for harmonic and reactive power compensation using pq theory". In: *2017 International Conference on Power and Embedded Drive Control (ICPEDC).* IEEE, 2017, pp. 260-264.
33. Belaidi, R., Haddouche, A., Fathi, M., Larafi, M. M., Kaci,, G. M., "Performance of grid-connected PV system based on SAPF for power quality improvement". In: *2016 International Renewable and Sustainable Energy Conference (IRSEC). IEEE,* 2016, pp. 542-545.

Nomenclature

BN	Brazilian Navy
CC BCU or C	Corveta Classe "Barroso"
Consumer Unit	
Δ_V	Variation of the voltage
EPQ	Electric Power Quality
EPS	Electrical Power System
h	Harmonic order
HP	Harmonic Pollution
I	Nonsinusoidal periodical instantaneous current
Ih	Harmonic instantaneous current
I1	Fundamental instantaneous current
IRPp-q	Instantaneous Reactive Power p-q
p	Instantaneous power active
q	Instantaneous power reactive
SAPF	Shunt Active Power Filter
TDD_I	Total Demand Distortion of current
THD_I	Total Harmonic Distortion of current
THD_V	Total Harmonic Distortion of voltage
V	Nonsinusoidal instantaneous voltage
V_1	Fundamental instantaneous voltage
V_h	Harmonic instantaneous voltage
VM	Voltage Modulation
V_{min}	Minimum Voltage
V_{max}	Maximum Voltage
V_n	Nominal Voltage
WCU Water Cooling Unit	